J. Fluid Mech. (1979), *vol.* 93, *part* 2, *pp.* 225–239
Printed in Great Britain

The influence of relaxation on shock detachment

By H. G. HORNUNG AND G. H. SMITH
Department of Physics, Australian National University, Canberra, Australia

(Received 12 July 1978)

By establishing that the length scale governing the detachment of a shock wave from a wedge is the distance from the leading edge to the sonic line, and by considering the view of observers with different length scales, it is predicted that the detachment distance increases gradually with wedge angle for relaxing flow and more rapidly in a perfect gas. Both of these features are confirmed by experiments in the free-piston shock tunnel. The influence of other length scales is discussed. The phenomenon is related to a relaxation effect in which a subsonic layer grows from the translational–rotational shock as the wedge inclination is increased beyond the frozen sonic point.

1. Introduction

A two-dimensional wedge placed symmetrically in a uniform supersonic flow supports an oblique shock wave which is attached to the leading edge if the wedge is sufficiently slender. In the vicinity of the leading edge, the oblique shock on a slender wedge is straight if the fluid is in thermodynamic equilibrium before and immediately after the shock and if the shock itself is thin compared with the observer's length scale. Under such circumstances the conditions throughout region B (see figure 1*a*) are uniform and may be determined from the shock jump conditions, that is, from the conservation and state equations. Take the flow speed, V_B, to be a representative property of region B. For a given deflexion δ of the flow through the shock the shock jump conditions give two possible solutions for V_B, of which the 'stronger', with smaller V_B, is usually only realized in practice when the shock is curved. It is convenient to map the flow into the velocity-deflexion plane (see figure 1*b*). The whole of region A maps into the point $A'(V_\infty, 0)$ and point $B'(V_B, \delta)$ represents the whole of region B. When the shock front segment bordering region B is straight, the flow deflexion angle, δ, at the shock is constant throughout B, and equal to the angle of inclination, δ_w, of the wedge face relative to the freestream direction. The curve in figure 1 (*b*) is called a shock locus and represents all possible states which may be reached from state A *via* an oblique shock. As the wedge angle δ_w is increased from zero, the point B' moves from A' along the shock locus towards the sonic point S at which V_B has decreased to the local speed of sound. At this point an important change occurs. Whereas, before, conditions in B were supersonic, so that signals from the trailing edge of the wedge were unable to travel upstream, and the flow pattern near the leading edge was devoid of a length scale, information about the finiteness of the wedge, that is about the length w, can now be communicated to the leading edge. The flow pattern responds to this situation by exhibiting a curved attached shock when B' lies slightly to the left of S. The region B is then no longer uniform, and B' only represents the post-shock flow at

0022-1120/79/4221-6430 $02.00

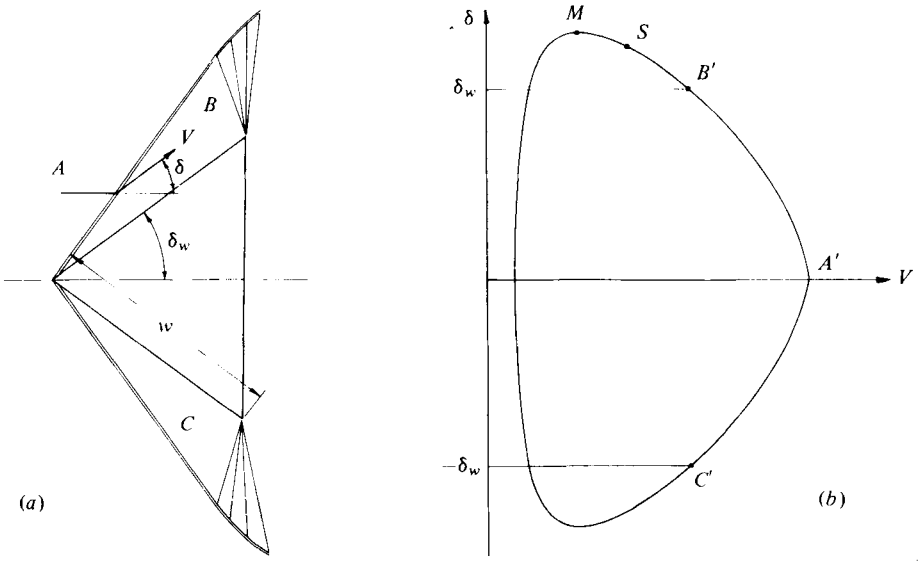

FIGURE 1. Attached shock wave and supersonic post-shock flow. (*a*) Physical plane. (*b*) V, δ plane. A, free stream; B, C, post-shock flow upstream of corner expansion; M, maximum deflexion point; S, sonic point. The flow near the leading edge is devoid of a length scale.

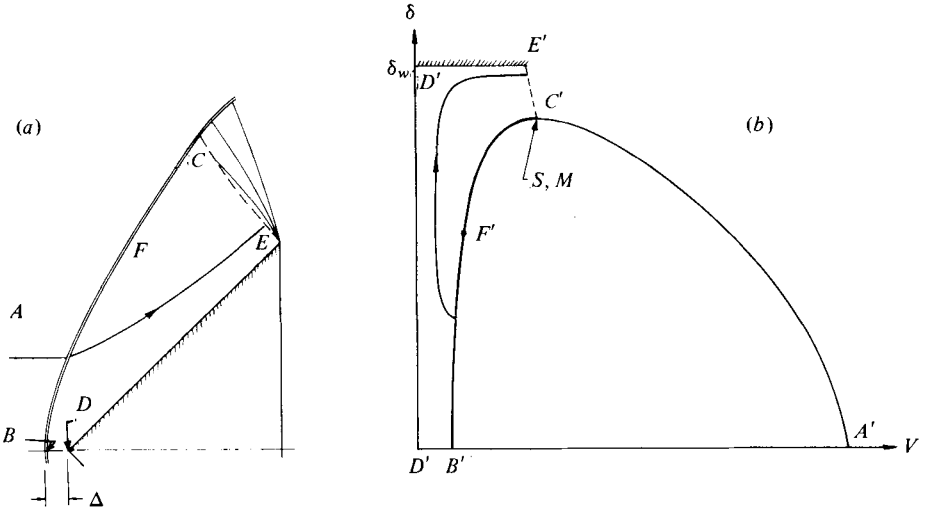

FIGURE 2. Detached shock wave and subsonic post-shock flow up to the sonic line at the trailing edge. (*a*) Physical plane. (*b*) V, δ plane. Information about the length scale w can reach the leading edge. S and M are effectively coincident at high free stream Mach number.

the leading edge, the remaining part of the shock being mapped into the portion of the shock locus between B' and S. For very large free stream Mach number, the case of present interest, the point S practically coincides with the maximum deflexion point M. When the wedge angle is increased beyond δ_M a significant change occurs in the flow pattern: The shock wave detaches from the leading edge of the wedge to form the flow pattern shown in figure 2(*a*) with the corresponding V, δ map of figure 2(*b*).

If S and M are considered to be coincident, a particular wedge angle $\delta = \delta_M$ sharply divides the two flow patterns of figures 1 (*a*) and 2 (*a*). In the former, the flow in region B is supersonic and 'knows' nothing about the extent of the wedge face; this results in the absence of a length scale in the flow pattern. In the latter case, the post-shock flow is subsonic, so that the length w communicates itself to all of the flow field over the wedge. For a given free stream and wedge angle the length scale of the flow pattern, as manifested for example by the stand-off distance Δ, is then proportional to w.

In the present investigation we inquire how the detachment process is modified when the approach to thermodynamic equilibrium at the shock occurs over a finite length, so that the equilibrium shock may no longer be considered thin. In the discussion of situations encountered in relaxation gas-dynamics it is convenient to introduce the smallest resolvable and largest viewable lengths of the observer, λ and Λ, say. The ratio Λ/λ is a measure of the range or power of observation. Let the relaxation lengths for translational, rotational, vibrational and dissociative relaxation be l_t, l_r, l_v and l_d respectively. In the following, vibration and dissociation will be regarded as a single relaxation process with characteristic length l. Similarly, translation and rotation may both be conveniently described by the length scale l_t. This is appropriate to the experimental conditions of § 3. The situation to be considered by an observer who cannot resolve any relaxation, is specified by the set of conditions

$$l_t < l < \lambda < w < \Lambda. \tag{1}$$

The shock observed by this observer will be referred to as 'equilibrium shock' for which the post-shock flow is everywhere seen to be in thermodynamic equilibrium. The case of present interest, in which the observer can resolve the dissociative relaxation, may then be specified by

$$l_t < \lambda < l < w < \Lambda. \tag{2}$$

Since our observer would regard as zero all lengths smaller than λ, (2) specifies a situation in which the translational shock thickness is zero. However, he can resolve dissociative relaxation, so that (chemical) equilibrium is reached within his window.

By restricting his field of view, Λ, the observer may reduce his power of observation and thereby change the nature of the problem he has to study, for example to

$$l_t < \lambda < \Lambda \ll l, \quad \Lambda \ll w. \tag{3a}$$

This corresponds to the case of a perfect or chemically frozen continuum gas in which the translational shock thickness is again zero. It is a set of assumptions appropriate for describing the conditions in the immediate vicinity of the frozen shock, before any appreciable dissociation has occurred. The gas may effectively be considered to be in a state of constrained equilibrium. For the observer (3) the post-shock equation of state is different from that for the observer (1), and consequently the shock jump condition and shock locus are also different; this is illustrated in figure 3. The region B, in a sufficiently small window $\Lambda(3)$, maps into the point B' on the 'frozen' shock locus (3) while the eventual equilibrium point C [well outside $\Lambda(3)$] maps into C' on the shock locus (1); this describes the flow when it has eventually attained chemical equilibrium; it may be thought of as the equilibrium shock locus.

The relative positions of the shock loci (1) and (3) are always as shown in figure 3 if the free stream is in unconstrained thermodynamic equilibrium, and the streamlines

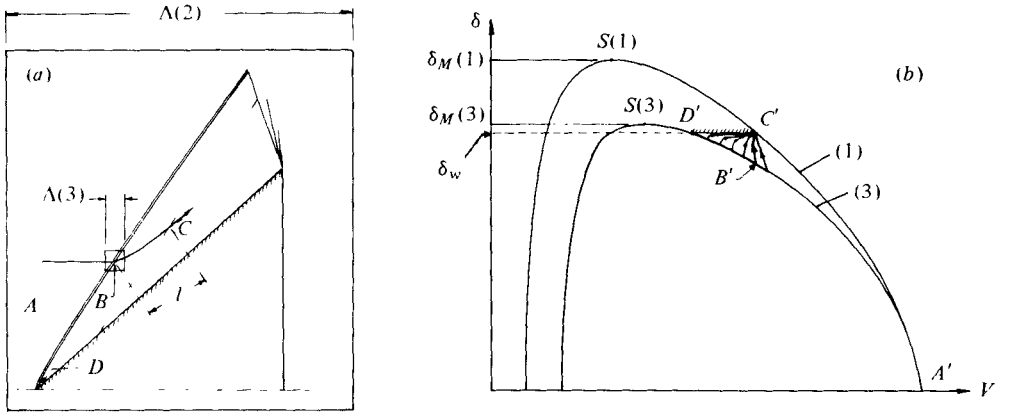

FIGURE 3. Flow over a wedge with resolvable relaxation length and an attached shock wave. (*a*) Physical plane. (*b*) V, δ plane. The shock loci seen by observers (1) and (3) do not coincide.

are drawn in the V, δ map according to the rules derived for relaxing flow by Hornung (1977). In the case illustrated in figure 3, the flow is supersonic everywhere.

In the above discussion the transition to observer (3) is made by holding the geometric length scale constant and varying the observer's length scale. This leads to observer (3) viewing a small part of a large experiment, the extent of which lies outside his window. He is therefore unable to measure w and cannot make any statements about the flow as a whole. If, on the other hand, the transition to observer (3) is made by increasing the relaxation length until it is much larger than Λ while maintaining the inequality $\Lambda > w$, he can view the perfect gas flow problem as a whole. His situation is then specified by

$$l_t < \lambda < w < \Lambda \ll l. \tag{3b}$$

It corresponds to the continuum, perfect gas situation commonly treated in gas dynamics text books.

It can now be demonstrated that detachment is a more complex process when the relaxation can be resolved by the observer. Consider the case when δ_W lies between the maximum deflexion angles $\delta_M(1)$ and $\delta_M(3)$ (see figure 4*b*). According to observer (1) who cannot resolve l, the equilibrium shock is straight and attached. However, according to observer (2), who can resolve details within the relaxation length l, the frozen shock is detached. The two observers can only be simultaneously right if the detachment occurs on such a small length scale that observer (1) cannot resolve it, but observer (2) can. The same conclusion is reached when it is recognized that a small subsonic region starts to grow from the frozen shock as the shock angle is increased beyond that corresponding to $\delta_M(3)$; a more detailed discussion follows in § 2.2. The distance to the sonic point is the determining length scale for the stand-off distance Δ.

On the basis of the above arguments it may be expected that the observer (2), who can resolve l, will see the following as he increases δ_w. At $\delta_M(3)$ the frozen shock becomes strongly curved near the tip and, as δ_w increases further, begins to detach gradually, Δ being approximately proportional to the smoothly increasing distance to the sonic line, until the sonic line reaches the end of the relaxation zone. This point corresponds to $\delta_w = \delta_M(1)$, and a further increase in δ_w results in a very rapid move-

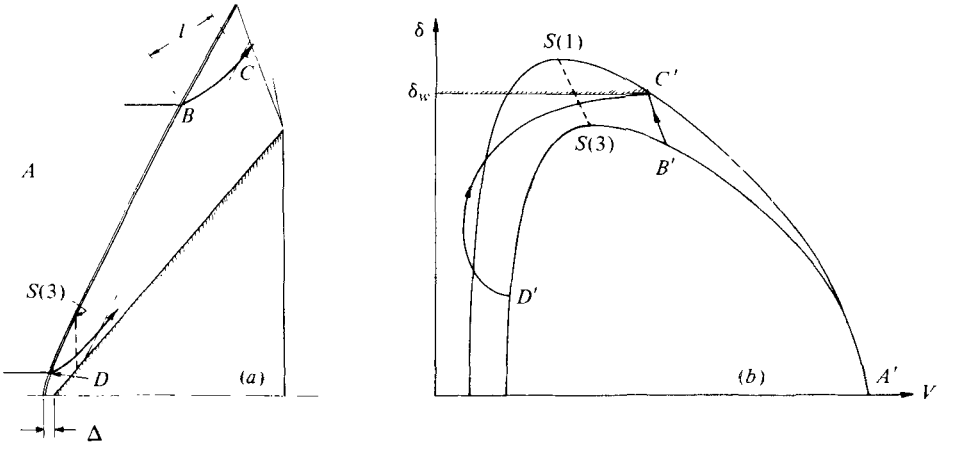

FIGURE 4. When $\delta_M(3) < \delta_w < \delta_M(1)$, observer (3) sees a detached shock, but observer (1) sees an attached shock. This can occur only if Δ is so small that observer (1) cannot resolve it. Note that the equilibrium shock locus (1) applies only if the shock curvature is small compared with $1/l$. (*a*) Physical plane. (*b*) V, δ plane.

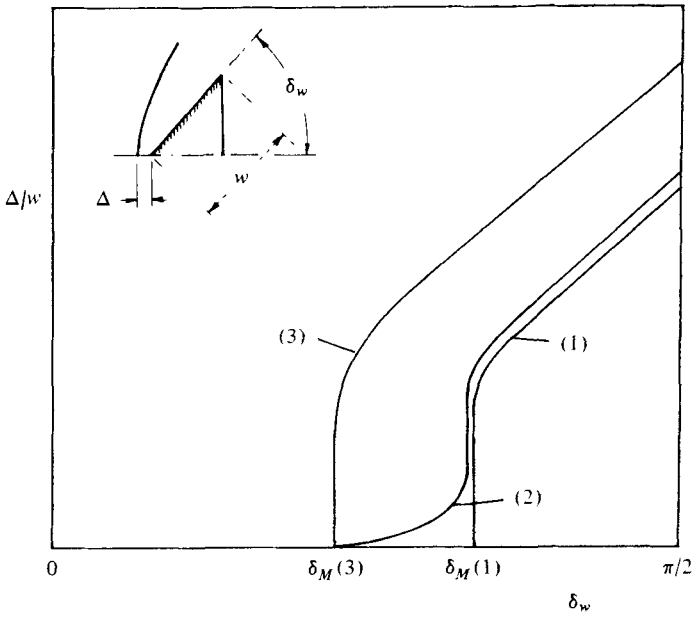

FIGURE 5. Behaviour of stand-off distance with wedge angle as predicted for observers (1), (2) and (3).

ment of the sonic line to the trailing edge of the wedge (see also figure 8*b*), and a consequent rapid increase in Δ. This corresponds to the detachment of the equilibrium shock. Figure 5 illustrates the variation of the stand-off distance with δ_w, expected by observers (1), (2) and (3). The behaviour of the curves as $\delta_w \to \frac{1}{2}\pi$ is sketched in according to the expectation that the stand-off distance, measured not from the tip but from the line joining the trailing edges of the wedge, becomes insensitive to δ_w as $\delta_w \to \frac{1}{2}\pi$ (see Cabannes 1960).

The aim of the present investigation is to test these predictions for observers (2) and (3) experimentally in the free-piston-driven shock tunnel with dissociating nitrogen and carbon dioxide flows, for which this facility is able to reproduce the conditions of observer (2) around the detachment angle. As a check, perfect gas argon flows should reproduce the conditions of observer (3) reasonably well.

2. Theoretical considerations

2.1. *Dimensional analysis*

In the dynamics of an inviscid perfect gas (frozen flow) with a uniform free stream the variables governing the flow over a body are the free stream speed, pressure and density, $V_\infty, p_\infty, \rho_\infty$, the ratio of specific heats, γ, the size of the model, w, say, and additional parameters describing the shape, such as the wedge angle δ_w in our problem. Thus, the shock stand-off distance Δ may be written in dimensionless form

$$\Delta/w = f_3(M_\infty, \gamma, \delta_w). \tag{4}$$

These are the variables that are important to observer (3) when w is within his window. M_∞ is the free stream Mach number $V_\infty \rho_\infty^{\frac{1}{2}}/(\gamma p_\infty)^{\frac{1}{2}}$.

For observer (1) the chemical composition changes (in zero distance after the shock), so that an additional variable is required to specify the flow completely. This may be conveniently chosen to be the amount of energy per unit mass, E, to bring the gas to its new equilibrium state at some representative condition, say after a normal shock. Hence, for observer (1),

$$\Delta/w = f_1(M_\infty, \gamma_\infty, \delta_w, \mu), \tag{5}$$

where $\mu = V_\infty^2/2E$, and γ_∞ is the ratio of specific heats in the free stream.

Observer (2) sees the composition change over a finite distance and therefore requires yet another variable to specify his picture completely, namely the relaxation length l. For him,

$$\Delta/w = f_2(M_\infty, \gamma_\infty, \delta_w, \mu, l/w). \tag{6}$$

The transition from the flow seen by observer (1) to that of observer (3) proceeds via that seen by observer (2) and may be described by

$$f_1 \to f_2 \to f_3 \tag{7}$$

corresponding to the change

$$0 \to l/w \to \infty. \tag{8}$$

For constant free stream conditions, the parameters M_∞, γ_∞ and μ are constant and may be omitted from f_1, f_2 and f_3. The problem of observer (2) then reduces to

$$\Delta/w = f(\delta_w, l/w), \tag{9}$$

the dependence on l/w disappearing for the other two observers, for whom only δ_w matters.

2.2. *The position of the sonic line*

Our motivation to study the detachment process in relaxing flow came about through our discovery that in relaxing flow through an oblique shock there exists a range of

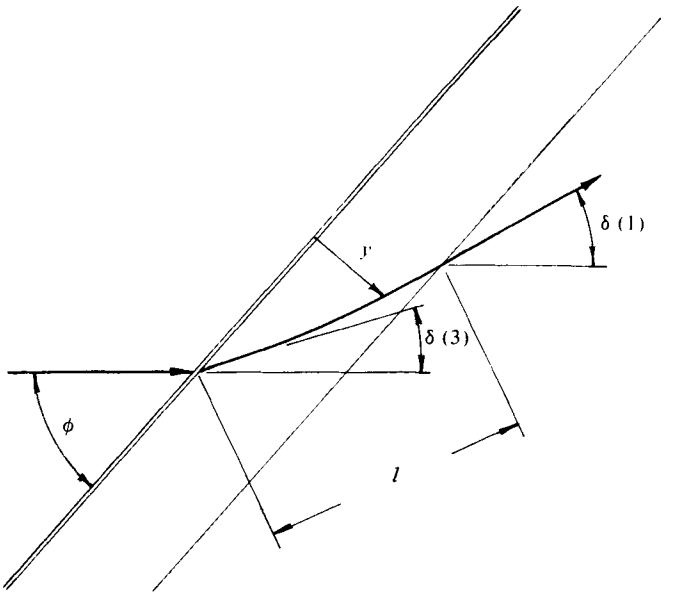

FIGURE 6. Notation for flow through a straight, oblique shock with relaxation.

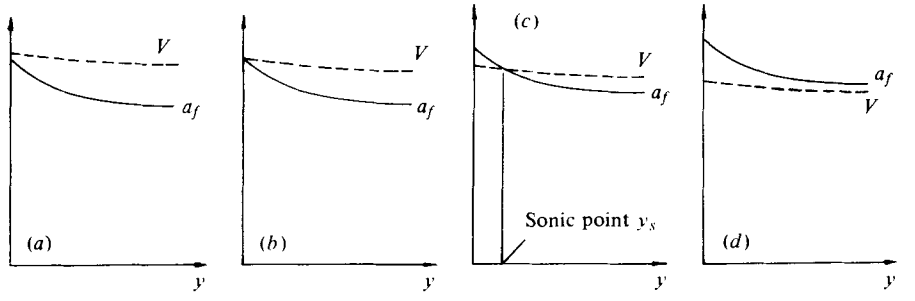

FIGURE 7. The growth of a subsonic layer after a straight, oblique shock making an angle ϕ with the free stream. (*a*) $\phi < \phi_s(3)$. (*b*) $\phi = \phi_s(3)$. (*c*) $\phi > \phi_s(3)$. (*d*) $\phi > \phi_{se}$. Relaxation causes the frozen speed of sound, a_f, to decrease more rapidly than the flow speed, V, with distance from the shock.

shock angles within which the flow after the translational shock is first subsonic and then becomes supersonic again within the relaxation zone. This is an effect which is of dominant importance to the detachment process. It comes about essentially because the frozen speed of sound, a_f, falls more rapidly than the flow speed, along a streamline within the relaxation zone.

In order to illustrate the effect it is convenient to consider a straight, oblique shock making an angle ϕ with the free stream, as shown in figure 6. The streamline is deflected by the translational shock to the frozen deflexion angle $\delta(3)$, and within the relaxation zone it suffers a further deflexion to the equilibrium deflexion angle $\delta(1)$. Let the distance measured at right angles to the shock be y. As ϕ is increased from a point where the flow is everywhere supersonic, the sequence of sketches of figure 7 illustrates the process by which a subsonic region grows from the translational shock to cover the

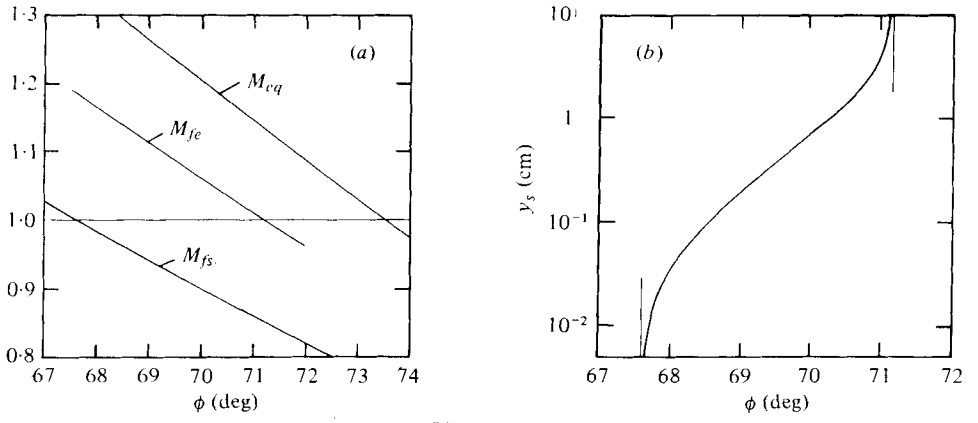

FIGURE 8. (*a*) Numerical calculations of dissociative relaxation of nitrogen after a straight oblique shock at a freestream speed of 6 km/s, showing the frozen Mach number at the shock, M_{fs}, and at the end of the relaxation zone, M_{fe}, as well as the equilibrium Mach number as functions of the shock angle ϕ. (*b*) The corresponding movement of the frozen sonic point away from the shock.

whole region downstream of the shock. The sequence relates ϕ to two of its possible values, one when the frozen shock becomes sonic, $\phi_s(3)$, and the other when the flow becomes sonic at the end of the relaxation zone, ϕ_{se}.

To substantiate this idea quantitatively, numerical calculations were made for a series of straight oblique shocks in a dissociatively relaxing nitrogen flow at fixed freestream conditions. (These conditions were chosen arbitrarily and do not represent those of the experiments in section 3 exactly.) The results are presented in figure 8. Figure 8(*a*) shows the frozen Mach number $M_f = V/a_f$, calculated at the translational shock (subscript *s*) and at the end of the relaxation zone, i.e. at the equilibrium composition (subscript *e*), plotted against the shock angle ϕ. As may be seen, the flow becomes sonic at the translational shock when $\phi = 67{\cdot}6°$ but becomes supersonic again within the relaxation zone for shock angles up to $\phi = 71{\cdot}2°$. At the former condition, $\delta(3) = 45°$ and, at the latter, $\delta(1) = 56°$, a change of 11° in the relevant wedge deflexion angle.

The corresponding distance to the sonic point, y_s, is shown in figure 8(*b*). The implication to the detachment process of the variation of y_s with ϕ is that signals from downstream of $y = y_s$ cannot reach the shock. It follows that the region of the flow field which is able to influence the flow near the tip of a wedge is the subsonic region of dimension y_s. The latter must therefore be the determining length scale for the stand-off distance Δ. As ϕ is increased through $\phi_s(3)$, observer (2) may therefore expect to see Δ increase smoothly like y_s. This behaviour is in agreement with that expected from the argument in the introduction and outlined in figure 5.

Figure 8(*a*) also shows the equilibrium Mach number $M_{eq} = V/a_{eq}$, where a_{eq} is the equilibrium speed of sound; a_{eq} is the speed at which disturbances of a wavelength much larger than l propagate and is smaller than the frozen speed of sound a_f, relevant for short wavelengths. Observer (1) cannot detect wavelengths shorter than l so that a_{eq} is the sound speed relevant to his observations. Both observers (3) and (2) must consider disturbances propagated at a_f, however, since they can resolve wavelengths shorter than l. The region downstream of the shock must therefore be considered to be

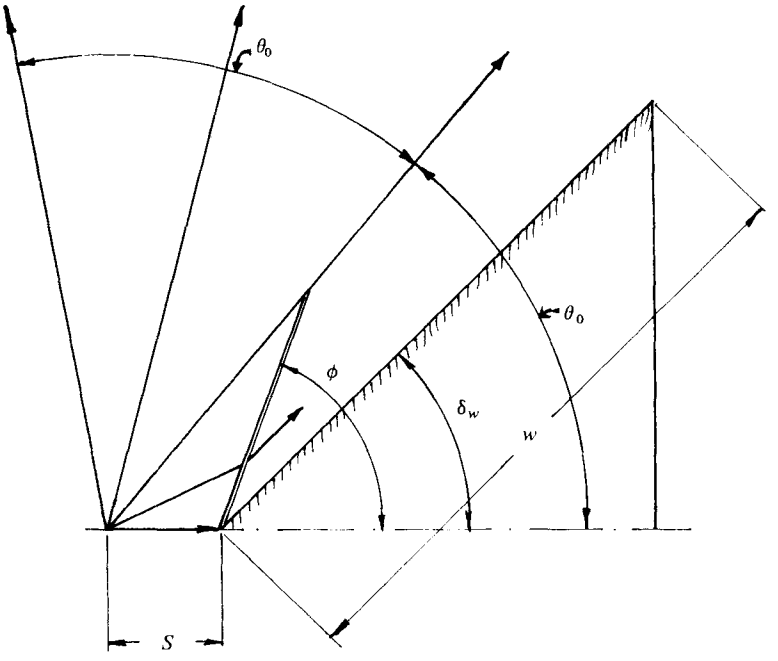

FIGURE 9. The source flow effect.

wholly subsonic above $\phi = 71{\cdot}2°$ in the example of figure 8, since we identify ourselves with observer (2).

2.3. *Other length scales*

Experience with the interpretation of interferograms of relaxing flows has shown that the presence of other length scales can produce phenomena which manifest themselves in a manner similar to relaxation. Care must therefore be taken to avoid such effects. To illustrate how thay may come about in the flow over a wedge, two specific additional lengths are considered in detail. These are the transverse length of the wedge, L, and the distance to the source point in a divergent free stream, S. The latter is important if, as is often the case, a conical nozzle is used to generate the flow.

The presence of these two additional lengths would alter (9) to the form

$$\Delta/w = f'(\delta_w, l/w, S/w, L/w). \tag{10}$$

These additional two parameters could make interpretation of experimental results much more difficult, so that it is desirable to produce a situation with $L/w = S/w = \infty$. The manner in which these two parameters affect our experiment may best be studied by considering the extreme cases $L/w \to 0$ and $S/w \to 0$.

Take $S/w \to 0$ first. For simplicity let the source flow have plane symmetry and consider a wedge of large flank length w, placed with its tip a small distance S from the source (see figure 9). Within a distance from the tip which is small compared with S, the flow is like that for a parallel free stream, producing a shock at an angle ϕ, say. Assuming this shock to be straight (for simplicity) and proceeding along it away from the tip, the streamlines cross it at smaller and smaller angles, so that the shock becomes progressively weaker, until, at $\theta = \theta_0$, it ceases to deflect the streamline. The mass

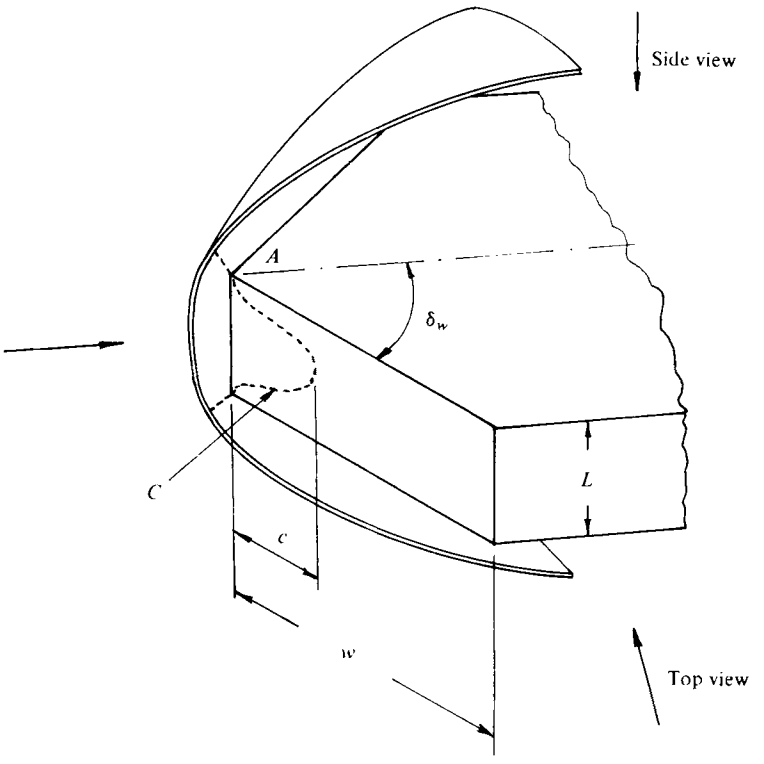

FIGURE 10. The effect of finite transverse length. Perspective view of model and cut-away shock.

flux between the wedge and $\theta = \theta_0$ is the same as that between $\theta = \theta_0$ and $\theta = 2\theta_0$, however the rate of increase of cross-sectional area in the latter sector is much larger. Consequently the pressure drops more quickly along the streamline in the sector $\theta_0 < \theta < 2\theta_0$ than near the wedge, and pressure-equalizing expansion waves cause the flow near the wedge to be accelerated. If the shock at the tip is detached, followed by subsonic flow, this acceleration can cause the flow to become supersonic before it encounters the trailing edge of the wedge. The sonic point may therefore reside on the face of the wedge rather than at the trailing edge. It is not necessary for the situation to be as extreme as that in figure 9 for the effect to be noticeable, as even a slight weakening of the shock at distances small compared with S can cause the necessary slight acceleration of the flow.

A similar effect may occur when the experiment is performed in an open jet. The wedge shock is reflected as an expansion wave from the edge of the jet. This expansion wave may impinge on the wedge face and cause the flow to be accelerated if the jet diameter, yet another length scale, is too small.

Finite L/w also causes the sonic line to move forward by a similar mechanism, with the accelerating expansion coming in from the side of the model. It may be illustrated by considering a wedge of finite width L in the extreme case $L/w \to 0$ when $\delta_w > \delta_M$, see figure 10. By considering the flow in the immediate vicinity of the tip, within a radius small compared with L, the shock is seen to be detached. However, when viewing the flow from the 'top', the symmetry plane containing the leading edge of the wedge

intersects the sonic surface in a line emanating from the end point A of the leading edge. The expansion propagating inwards from the sides accelerates the flow and causes the sonic surface to intersect the wedge face in a curve C, whose maximum extent c from the leading edge is smaller than w.

Other effects such as the displacement due to a viscous boundary layer can cause the wedge face to be effectively convex. This too would bring the sonic point closer to the leading edge.

The above discussion shows that many finite lengths, some of which are unavoidable in an experiment, produce effects similar to those of relaxation. It is therefore essential that any experiment examining the effect of relaxation must be complemented by a control experiment in which the relaxation effect is removed (e.g. by making $l/w \to \infty$) while the other finite length scales are retained.

3. Experiment

3.1. *Facility, model and instrumentation*

Much of the discussion in the preceding section about length scales other than l and w arose in the first place because a pilot experiment for this project had been performed in the small free-piston shock tunnel at A.N.U. (known as T2). In these experiments the nozzle was conical ($S/w \simeq 4$), the wedge face length was comparable to the free jet diameter, and the transverse length of the model was such that $L/w \simeq 1$. An asymmetric wedge was used, consisting of a flat plate whose incidence was adjusted to change δ_w. The experiment measured the stand-off distance as a function of δ_w for reacting nitrogen and carbon dioxide as well as perfect gas argon flows.

In view of the importance of L/w and S/w in this experiment, it is not surprising in hindsight that the results were inconclusive, inasmuch as the behaviour of Δ/w with δ_w had essentially the same features for the perfect gas argon flow as for the dissociating flows, all of which showed a gradual increase of Δ/w with δ_w.

In order to reduce the undesirable effects of finite L/w and S/w, the experiment was performed again in the large free-piston shock tunnel, T3 (see Hornung & Stalker 1978) with a contoured nozzle and also with a symmetrical wedge. This contoured nozzle was originally designed for use with air at a specific reservoir enthalpy of 3×10^7 m^2/s^2 and a reservoir pressure of 200 atm. However, it also gives good quality parallel, uniform flows ($S/w = \infty$) with specific reservoir enthalpies in nitrogen of $2{\cdot}2 \times 10^7$ m^2/s^2, carbon dioxide of $1{\cdot}6 \times 10^7$ m^2/s^2 and argon of $2{\cdot}5 \times 10^6$ m^2/s^2. The former two gases are partially dissociated in the reservoir and recombine rapidly as they cool upon flowing through the throat, while their composition is frozen by the rapid drop in density through the nozzle flow. The effective specific heat ratios, and therefore the exit Mach numbers, are different for the two gases. At the low enthalpy chosen for the argon, it behaves like a perfect gas. Though the nominal exit Mach number is 16 for the argon flow, the displacement thickness of the nozzle wall boundary layer is quite large at this condition, so that the exit Mach number may be significantly reduced. The test section conditions for the three gases are obtained by numerical computation of the nozzle flow from the measured reservoir conditions and are given in table 1.

The new model consisted of two sharp wedges whose position and incidence could be

	Nitrogen	Carbon dioxide	Argon
Specific reservoir enthalpy (m^2/s^2)	$2{\cdot}2 \times 10^7$	$1{\cdot}6 \times 10^7$	$0{\cdot}25 \times 10^7$
Reservoir temperature (K)	9070	5750	5000
Reservoir pressure (atm)	180	180	180
Exit velocity (km/s)	5·5	4·1	2·2
Exit density (g/cm^3)	$2{\cdot}6 \times 10^{-6}$	$4{\cdot}6 \times 10^{-6}$	$2{\cdot}2 \times 10^{-6}$
Exit temperature (K)	1100	1960	57
Exit Mach number	7·5	6·0	16
Exit composition (mole/g)	N_2 0·0319 N 0·0077 $e^- < 10^{-6}$ $N^+ < 10^{-6}$	$C < 10^{-10}$ O 0·0044 CO_2 0·0074 O_2 0·0055 CO 0·0153	Ar 0·025

TABLE 1. Calculated tunnel conditions.

adjusted separately so that they could be arranged in the form of a single symmetrical wedge with variable δ_w by making their leading edges touch. Small nonuniformities in the leading edges caused a gap of no more than 0·2 mm width to appear between the leading edges. This was sealed from behind the wedges with a pliable vacuum-sealing compound. The width of the model was $L = 15{\cdot}2$ cm and w was 5·1 cm giving $L/w = 3$. This is still quite finite and should ideally be much larger. However, at the chosen conditions the relaxation length is approximately 1–2 cm, and the exit diameter of the nozzle is 25 cm. In order to stay well clear of the edge of the free jet it is necessary to have L sufficiently small compared with 25 cm ($L = 15{\cdot}2$ cm chosen). To produce a behaviour significantly different from the frozen flow of observer (3) it is desirable to make l comparable to w. This led to the compromise $w = 5{\cdot}1$ cm, i.e. $l/w \doteqdot \frac{1}{3}$, $L/w = 3$.

The flow was investigated by Mach–Zehnder interferometry, the light source being an exploding wire. This produces a sufficiently short ($\sim 50\,\mu$s) intense light pulse, bright enough to overcome the self-luminosity of the gas in the shock layer, which is also partially eliminated by a stop at the exit focus of the interferometer and by an interference filter passing wavelengths of 510 ± 5 nm. The main purpose of the filter is to facilitate quantitative interpretation of the interferograms.

3.2. *Results*

As an example of the experimental results obtained with a relaxing flow, a set of interferograms of dissociating carbon dioxide flow over the wedge is presented in figure 11. These show an attached shock in figure 11(*a*), and gradually increasing stand-off distance with increasing δ_w through to figure 11(*e*). Figure 11(*a*) shows a curved attached shock followed by strong relaxation as indicated by the decrease of fringe shift gradient with distance from the shock. The sharp rise in fringe shift at the wedge surface is due to the boundary layer and gives an indication of its thickness.

Two examples of detached shocks in argon are presented in figure 12. In these interferograms the trailing edge of the wedge is obscured by a support bracket on the side of the wedge which does not significantly affect the flow over the wedge. Notice the

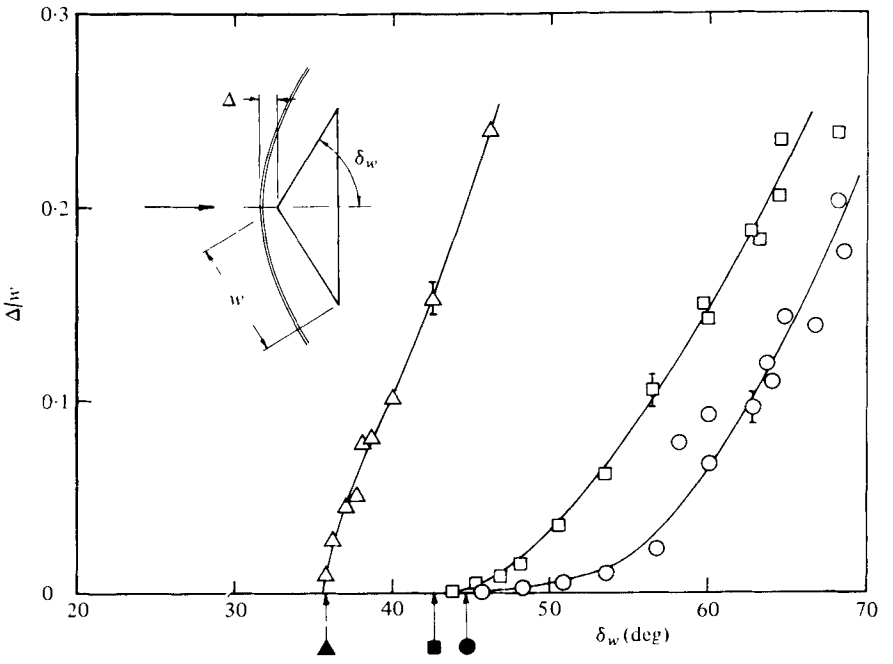

FIGURE 14. Measured stand-off distance for: △, the perfect gas argon; □, dissociating nitrogen; ○, dissociating carbon dioxide. For freestream conditions see table 1. The filled symbols indicate the calculated frozen detachment angle. The curves are mean lines through the experimental results.

more nearly constant fringe shift in the shock layer, indicating a more uniform density field. Also, the boundary layer on the wedge surface is noticeably thicker than in the carbon dioxide flows. Figure 12 (*a*) shows a situation with δ_w barely above the incipient detachment angle and figure 12 (*b*) shows a case with Δ so large that it can be appreciated that finite L/w and finite open jet diameter will affect the results.

Incipient detachment and a small Δ are shown for dissociating nitrogen flow in figures 13 (*a*) and (*b*). Again a considerable change in δ_w is necessary to change Δ relatively slightly.

The features of the interferograms taken at the three conditions of table 1 are presented in figure 14, which is a graph of Δ/w against δ_w. Estimated error bars for the measurement of Δ are indicated on a few representative points, while the error in δ_w is smaller than the size of the symbols. There are a few points showing a significant discrepancy from the main trend in the carbon dioxide data, which we are unable to explain. The value of $\delta_M(3)$, the frozen detachment angle, as calculated from the freestream conditions is also shown in figure 14, and may be seen to agree well with the observed incipient detachment point in all three cases.

It is shown in figure 14 that the trend at small values of Δ/w is as expected from the argument in the introduction. The relaxing flows give a very slow rise of Δ/w with increase of δ_w, whereas the perfect gas flow gives a rapid increase.

4. Discussion

The perfect gas detachment process has been examined by a number of authors whose results indicate that Δ/w increases gradually with δ_w even in the absence of relaxation. Guderley (1962) obtains this result on theoretical grounds; Frank (1972) from measurements in transonic flows; Zierep (1968) from similarity arguments; and Johnston (1953) from measurements at $M_\infty = 2{\cdot}5$. The former three are concerned with the transonic situation in which the sonic and maximum deflexion points on the shock locus (S and M) are significantly separated. In Johnston's results the gradient $d\Delta/d\delta_w$ at incipient detachment is comparable with that of the present experiments at $\Delta/w \approx 0{\cdot}1$ in argon. However, following the argument presented in the introduction, we observe that, in parallel, frozen flow with $L/w = \infty$, no length scale is available to the flow at the tip of the wedge until the flow becomes subsonic after the shock. At high Mach number, M and S effectively coincide, so that, at incipient detachment, the length scale governing the stand-off distance jumps from zero to w. It is probable that, in the absence of relaxation, any smoothing of the effect of this discontinuity in the length scale on the behaviour of Δ with δ_w occurs because of finite L/w. The importance of this effect may be expected to increase as Δ/L increases. It is supported by the argon curve in figure 14. A possible way of testing this explanation is to repeat the experiment in frozen flow with a smaller w. This would reduce the importance of L/w in the frozen case.

5. Conclusions

The discussion of relaxing flows in terms of the phenomena seen by observers with different smallest resolvable and largest viewable length scales has been shown to give correct predictions in the case of detachment of a shock from a wedge. The mapping of the flow into the speed–deflexion plane has been shown to be a useful tool for obtaining the principal features of relaxing gas flows. The determining length scale for the detachment distance is the distance to the sonic line which has been shown to grow with increasing shock angle, even for a straight shock. The detachment distance therefore grows gradually as the wedge angle is increased for relaxing gases and more steeply for a perfect gas. Both features have been confirmed by experiment. The effect of finite transverse extent of the wedge and of a divergent free stream have been discussed and shown to produce similar effects as those due to relaxation.

The facility used in this project was financially supported by the Australian Research Grants Committee. The project has benefited greatly from discussions with Professor E. Becker during his visit to A.N.U.

REFERENCES

CABANNES, H. 1960 In *Handbuch der Physik*, vol. 9, p. 162. Springer.

FRANK, W. 1972 Dissertation, Karlsruhe.

GUDERLEY, K. G. 1962 *Theory of Transonic Flow*. Pergamon.

HORNUNG, H. G. 1977 *Proc. 6th Austral. Hydr. Fluid Mech. Conf. Adelaide*, pp. 217–220.

HORNUNG, H. G. & STALKER, R. J. 1978 In *Applied Fluid Mechanics* (ed. H. Oertel), Karlsruhe University.

JOHNSTON, G. W. 1953 *J. Aeron. Sci.* **20**, 378–382.

ZIEREP, J. 1968 *Acta Mechanica* **5**, 204–208.

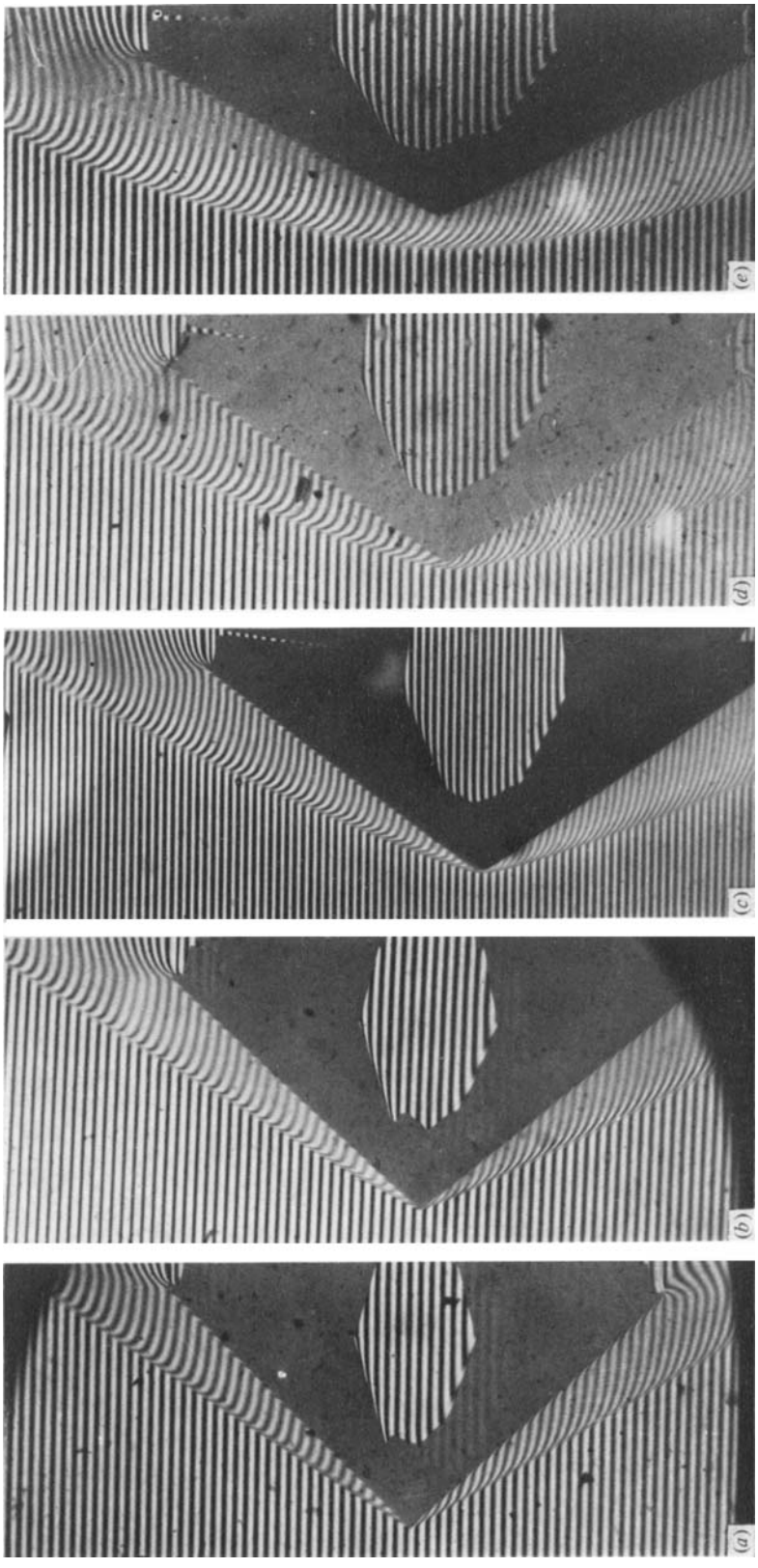

FIGURE 11. Interferograms of dissociating carbon dioxide flow over a wedge. (*a*)–(*e*) show progressively larger wedge angles with increasing detachment distance. For freestream conditions see table 1.

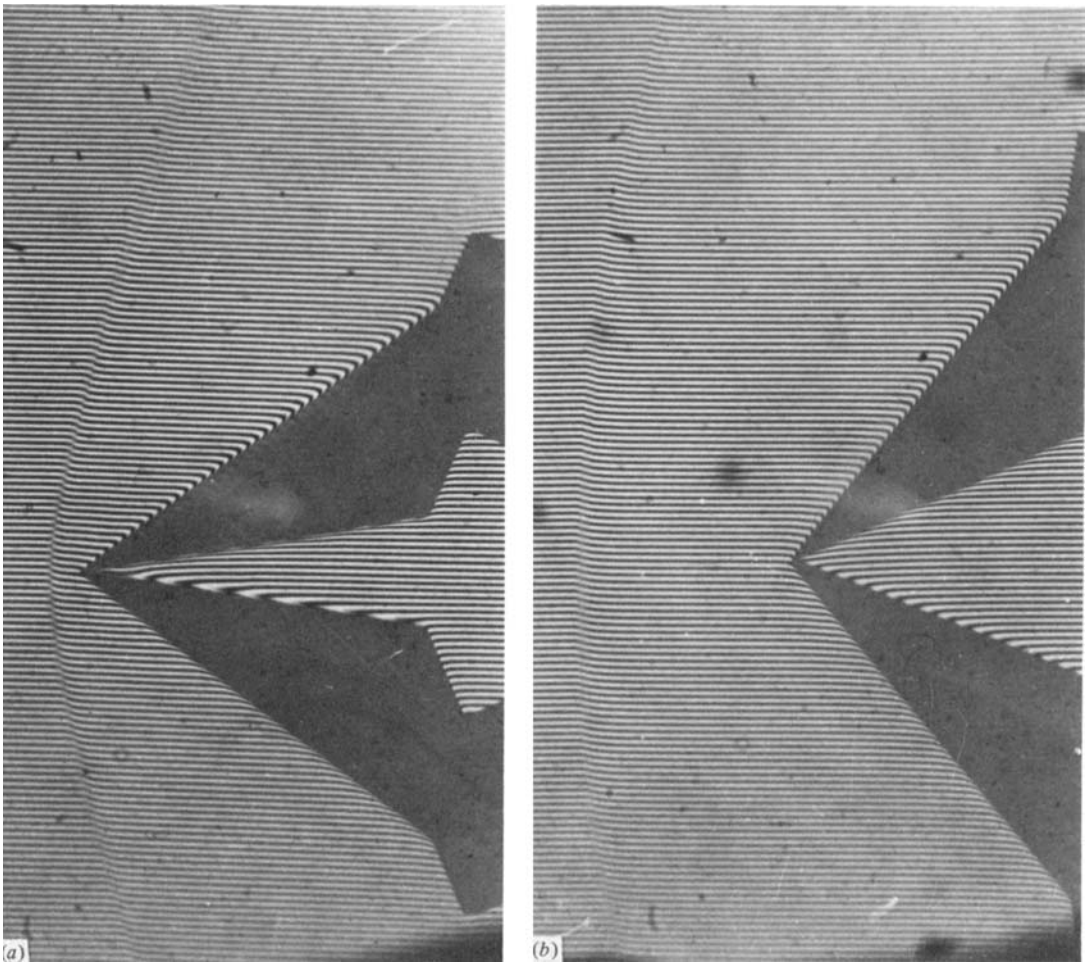

FIGURE 12. Interferograms of perfect gas flow (argon) over a wedge. (*a*) Just detached shock. (*b*) Large stand-off distance. For freestream conditions see table 1.

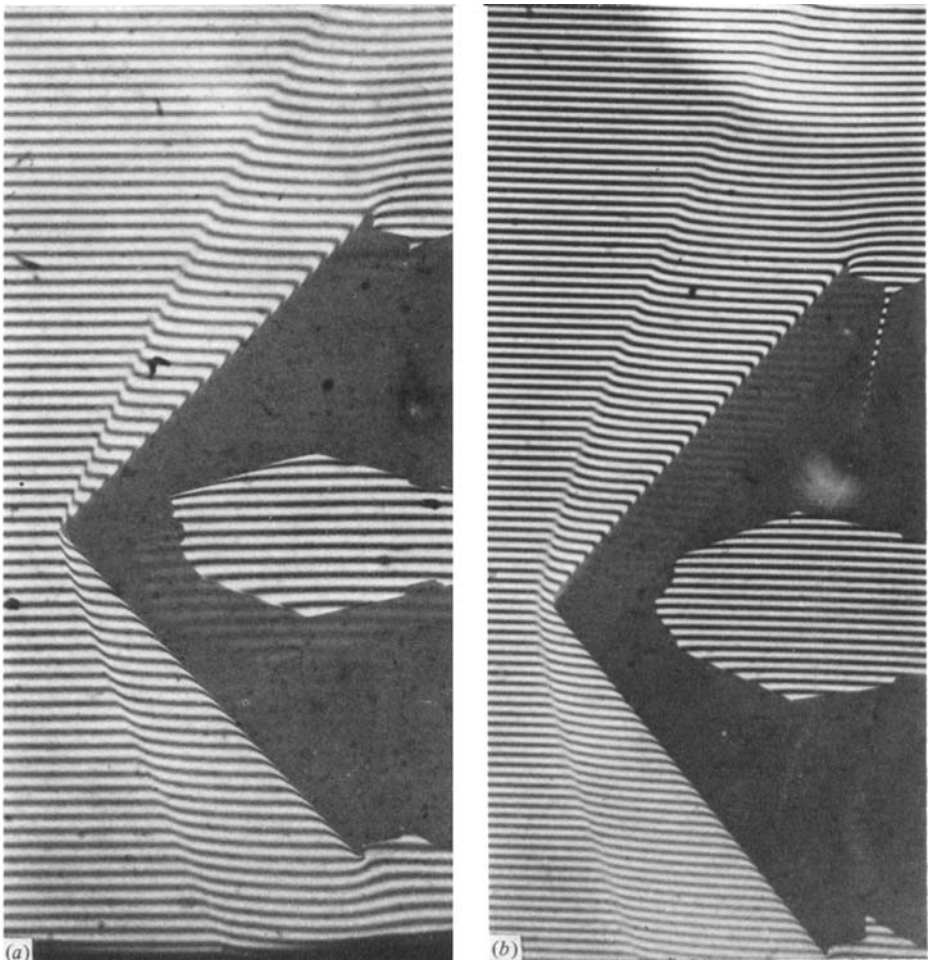

FIGURE 13. Interferograms of dissociating nitrogen flow over a wedge. (*a*) Curved attached shock. (*b*) Small stand-off distance. For freestream conditions see table 1.